LONG-PERIOD EARTHQUAKE SIMULATIONS IN THE WASATCH FRONT, UT: MISFIT CHARACTERIZATION AND GROUND MOTION ESTIMATES

Morgan P. Moschetti
US Geological Survey
Golden, CO 80401
USA

Leonardo Ramirez-Guzman
US Geological Survey
Golden, CO 80401
USA

ABSTRACT

In this research we characterize the goodness-of-fit between observed and synthetic seismograms from three small magnitude (M3.6-4.5) earthquakes in the region using the Wasatch Front community velocity model (WCVM) in order to determine the ability of the WCVM to predict earthquake ground motions for scenario earthquake modeling efforts. We employ the goodness-of-fit algorithms and criteria of Olsen and Mayhew (2010). In focusing comparisons on the ground motion parameters that are of greatest importance in engineering seismology, we find that the synthetic seismograms calculated using the WCVM produce a fair fit to the observed ground motion records up to a frequency of 0.5 Hz for two of the modeled earthquakes and up to 0.1 Hz for one of the earthquakes. In addition to the reference seismic material model (WCVM), we carry out earthquake simulations using material models with perturbations to the regional seismic model and with perturbations to the deep sedimentary basins. Simple perturbations to the regional seismic velocity model and to the seismic velocities of the sedimentary basin result in small improvements in the observed misfit but do not indicate a significantly improved material model. Unresolved differences between the observed and synthetic seismograms are likely due to un-modeled heterogeneities and incorrect basin geometries in the WCVM. These differences suggest that ground motion prediction accuracy from deterministic modeling varies across the region and further efforts to improve the WCVM are needed.

INTRODUCTION

The Wasatch Front (WF) is home to more than 2 million people and stretches for more than 200 km in northeastern Utah (UT). Formed by displacements across the predominantly normal-faulting Wasatch fault, which has generated more than 2000 m of topographic relief, the front separates the Wasatch Range, to the east, from a series of sedimentary basins that have formed in the down-dropped hanging-wall block. Basin sediments include consolidated, semi-consolidated and unconsolidated materials, including very low seismic velocity lacustrine, fluvial and deltaic sediments from Lake Bonneville. The basin boundaries encompass the urban centers of Salt Lake City, Ogden and Provo, UT (see Fig. 1).

Although large earthquakes (M≥7) have not occurred during the historical period, the paleoseismological record indicates the occurrence of 16 events in the past 5600 years, for an average earthquake repeat time of 350 years (McCalpin and Nishenko, 1996). Six segments comprise the fault (Lund, 2005); repeat times for the five central segments range between 1200-2600 years and pose a 16 and 30% probability of ocurring for 50 and 100 year exposures, respectively (McCalpin and Nishenko, 1996). Because of the proximity of more than 80% of Utah's population to the Wasatch fault and the likelihood of future large earthquakes, there is a need to estimate the earthquake ground motions that might be expected in the region. The potential for a large (M≥7) earthquake on the Wasatch fault greatly increases the seismic hazard in the Wasatch Front, UT region. Because no seismic records from large earthquakes are available for this area and complex effects on the earthquake ground motions from sedimentary basins are expected, on-going efforts are being made to estimate potential ground motions.

Various approaches may be taken to characterize the seismic hazard in this, and other, regions. The standard practice for estimating the ground motion levels from a fault at a location of interest for a given earthquake magnitude is the use of ground motion prediction equations (GMPEs). Few records from normal-faulting events, mechanisms expected in the Wasatch fault, are available for inclusion in current GMPEs. As a result, the ground motions from this fault may not be appropriately represented by these calculations. In

addition, the basin structures and very slow sediments within the basins west of the Wasatch Front add complexity to the regional wave propagation. Large earthquake ground motions within sedimentary basins have been shown to result from wave amplification, basin-edge effects, surface-wave scattering and hanging wall effects (e.g., Frankel et al., 2001; Olsen et al., 1995; O'Connell et al., 2007), all of which are difficult to incorporate into GMPEs. On the other hand, due to the increasing computational capacity, an alternate approach to characterizing earthquake hazards is to simulate potential earthquakes via numerical simulations in fully heterogeneous 3-D seismic velocity models. We utilize this approach in the current study.

The 3-D Wasatch Front community velocity model (WCVM) for the region (Magistrale et al., 2008) is currently being used by various groups for deterministic modeling of earthquake ground motions. Like other community velocity models, such as those for southern California (Magistrale et al., 2000; Suss and Shaw, 2003), Seattle (Stephenson, 2007), and the New Madrid seismic zone (Ramirez-Guzman et al., 2010), the WCVM is constructed from multiple data sources and types. Experience in modeling long period (f≤1.0-Hz) waveforms suggests that the most important elements of the model are the basin surface, sediment seismic velocities and the regional crustal and upper mantle seismic velocity model. Research groups from San Diego State University/University of Utah (Roten et al., 2010), Carnegie Mellon University (Taborda et al., 2010), University of California at Santa Barbara (Liu et al., 2010) and the US Geological Survey (Moschetti and Ramirez-Guzman, 2011) are carrying out earthquake ground motion simulations using the WCVM to characterize seismic hazard in the Wasatch Front region. The results of this collaboration will be incorporated into an urban seismic hazard map to provide higher-resolution seismic hazard values than are available in the national seismic hazard maps (Petersen et al., 2008).
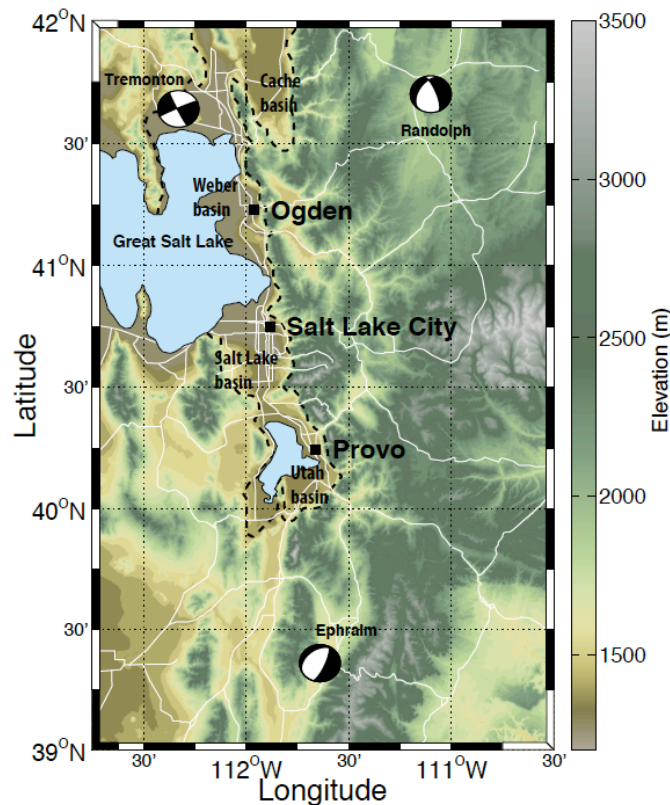

Fig. 1. Wasatch Front region. Elevation is plotted in meters above sea level. The surface trace of the sedimentary basins included in the WCVM is plotted with a dashed black line. Earthquake locations and focal mechanisms are displayed with beach-ball plots.

Although the results from these simulations will be incorporated into an urban seismic hazard map for the Salt Lake County region, a comprehensive validation of the seismic material model that is utilized for earthquake simulations has not been performed. This paper examines the ability of the WCVM to predict ground motions from three small earthquakes that were recorded in the WF region. Synthetic seismograms are compared with observed records in various frequency bands, and waveform parameter misfit is quantitatively analyzed. In addition, we simulate the scenario earthquakes using three alternate material models, which are constructed by simple perturbations to the WCVM. Other research groups have performed computationally-intensive inversions to improve the waveform fits from earthquake simulations using community velocity models (e.g., Tape et al., 2010); however, such approaches

require better broadband station coverage and greater numbers of moderate-sized earthquake records than are available for the WF region. In this paper we investigate whether simple model perturbations can improve the fit of synthetic seismograms to observed records.

METHODS

Material Model

The principal components of the WCVM, version 3c, are the stratigraphic surfaces (R1, R2 and R3) (see Fig. 2) that define velocity boundaries of the sedimentary basins, shallow seismic velocities from various seismic and geotechnical measurements, a background seismic velocity model from P-wave tomography and variable Moho depth. The stratigraphic surfaces R1 and R2 are identified from borehole measurements and refer to the boundaries between unconsolidated and semi-consolidated sediments and between semi-consolidated and consolidated sediments, respectively. The R3 surface gives depth to the sediment-basement boundary, which is estimated from gravity modeling and reflection and refraction studies (Bashore et al., 1982; Mabey et al., 1992; Mattick, 1970; McNeil and Smith, 1992). Sediment depths extend to more than 2 km over large regions within the modeled basins, as shown in Fig. 2. Within the sedimentary basins, seismic velocities are given by a weighted average of local velocity estimates from surface seismic and borehole measurement and empirical relations between sediment age and depth to seismic velocity. The WCVM employs the empirical relation from Faust (1951) for P-wave velocities in the sedimentary basins below the R1 interface:

$$V_P = k(da)^{1/6} \,. \tag{1}$$

where the coefficient, k (see Eqn. 1), is calculated to match observed P-wave velocities from deep-borehole measurements and d and a represent the sediment depth and age, respectively.

S-wave velocity and density are calculated from the estimated P-wave velocity by empirical relations (e.g., Magistrale et al., 2000). Outside of the sedimentary basins, a sonic-log-derived near-surface velocity profile tapers into the regional model. The near-surface profile has the effect of reducing the nonphysical seismic velocities given by the regional tomography at the model surface. The Salt Lake, Weber, Cache and Utah basins are modeled in the WCVM; currently, no other basin structures are included.

We use the attenuation model of Brocher (2006) for all Wasatch earthquake simulations, as used by Magistrale et al. (2008) in their simulation tests to the WCVM. Attenuation values are derived from S-wave velocities as:

$$Q_S = 13, V_S < 0.3 \text{ km/s} \tag{2}$$

$$Q_S = -16 + 104.13V_S - 25.222V_S{}^2 + 8.2184V_S{}^3, \, V_S \geq 0.3 \text{ km/s} \tag{3}$$

$$Q_P = 2Q_S \tag{4}$$

In addition to the simulations calculated with the WCVM, we simulate the set of earthquakes for three alternative material models, in which we make simple modifications to the WCVM. The alternate models include perturbations to the regional model and to the deeper basin structure, which we define as the basin volume between the R1 and R3 surfaces. We replace the regional velocity model, which is derived from P-wave tomography, with a velocity model derived from ambient noise tomography (Moschetti et al., 2010). We increase and decrease the coefficient, k, in Faust's rule by 10% to account for uncertainties in the estimation of deep basin velocities. The three alternate models are referred to as: (1) WCVM-ANT, where the regional model is replaced, (2) WCVM-b1, where the deep-basin shear-velocities are uniformly perturbed by -10% and (3) WCVM-b2, where the deep-basin shear-velocities are uniformly perturbed by +10%.

Earthquake Ground Motion Simulations

Elastic wave propagation is modeled by the finite element tool-chain Hercules (Tu et al., 2006). The tool-chain meshes the simulated domain, partitions the mesh and solves the wave propagation equations using an octree-based meshing strategy, which allows variable resolution that depends on the local seismic velocity. A minimum S-wave velocity of 200 m/s is used for the simulations. At the locations where the material wave speeds are below this threshold, we increase the S-wave velocity to the minimum value and preserve the initial Vp/Vs ratio. In the current implementation of the finite element solver, attenuation is modeled using Rayleigh damping. Wave propagation is simulated for a ground motion duration of 200 s. Earthquake records from seismographs located within the simulation domain indicate that this duration captures the direct arrivals and large amplitude coda waves that are of importance in

characterizing seismic hazard. The minimum simulation domain measures 130 km x 260 km x 65 km. Small variations in the size of the simulation domain exist between earthquake simulations to account for variation in epicenter locations and to ensure that the ground motions within the basins of WCVM are captured.
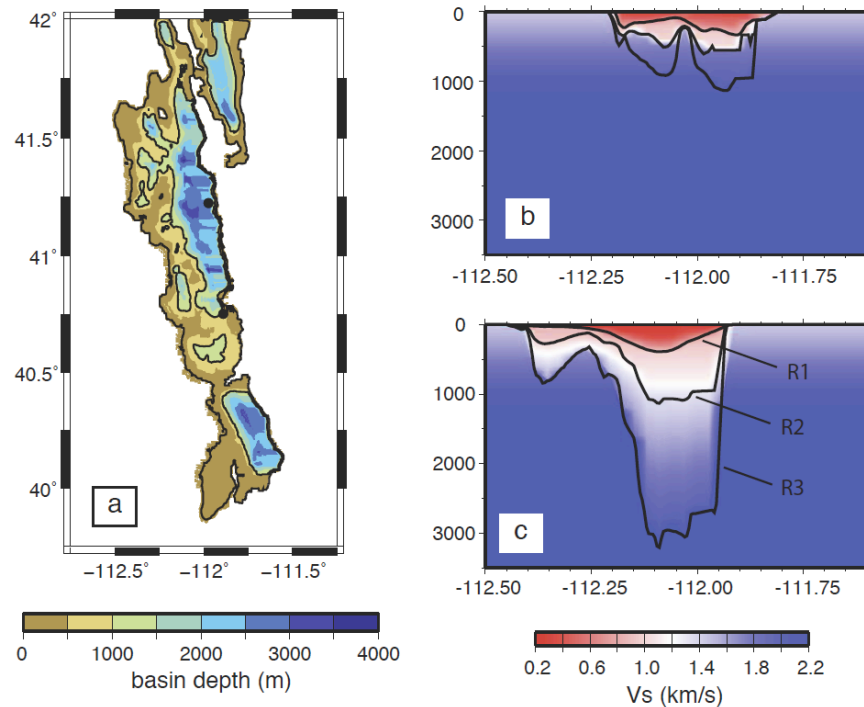

Fig. 2. Wasatch Front community velocity model (WCVM). (a) Basin depth in the WCVM. The outer and inner black contours represent 5 m and 1000 m sedimentary depths, respectively, and within them additional depth boundaries are color coded. Outside of the basin, seismic velocities are determined by the near-surface velocity profile and the regional seismic velocity model. Examples of the seismic velocity model at the latitudes of (b) 40.7° and (c) 41.2° N, corresponding to the approximate latitudes of Salt Lake City and Ogden, UT, respectively. Black solid lines in panels (b) and (c) identify the R1, R2 and R3 surfaces.

Earthquake simulations using the WCVM are carried out in the 0-1.0 Hz frequency band, using nine points per wavelength. Due to the large number of computing hours required to make the computations to 1.0 Hz and the modest improvements to waveform fits that we discuss below, we calculate the ground motions for the alternate seismic velocity models to 0.5 Hz. Simulations are carried out at the Teragrid computing facility, Kraken, and require between about 3,000-21,000 computing hours; the finer elements required to model higher frequency wave propagation result in computational times for the 1 Hz simulations that are more than seven times greater than the times for the 0.5 Hz simulations.

Simulated earthquakes and records

The epicenters of the three scenario earthquakes are located near the towns of Ephraim, Randolph and Tremonton, UT, and we refer to these earthquakes hereafter by their respective place names. Earthquakes with similar magnitudes (M>3.6) are relatively infrequent in the WF region; fewer than 15 events with magnitudes greater than 3.5 occurred between 2001 and 2010. Scenario earthquakes were selected to provide good azimuthal coverage of the seismic energy crossing the sedimentary basins in the WCVM and, for the case of the Tremonton and Ephraim events, to take advantage of the additional broadband instruments deployed as part of the USArray Transportable Array (TA).

Earthquake focal mechanisms are taken from the Moment Tensor Project for North America (Herrmann et al, 2011), and source parameters are summarized in Table 1. Because the earthquake magnitudes are uniformly less than M5, the earthquakes are treated as point sources. The double couple representing the source is implemented in the finite element solver by an equivalent set of forces within the element containing the point source; see e.g. Tu et al. (2006). We use a triangle slip-rate function with a rise time of 0.25 s, which has almost flat spectral amplitudes at the frequencies of interest.

The synthetic seismograms are compared with observed seismograms obtained from the University of Utah Seismograph Stations (UUSS) and the Advanced National Seismic Stations (ANSS). In addition, the Ephraim and Tremonton events occurred during the time that the TA was deployed in Utah, and additional broadband seismic records are available. UUSS and ANSS maintain 6 broadband, 34 short-period and 40 strong-motion seismographs within the simulation domain. During the TA deployment, 8 additional broadband instruments were available. Computational limitations for the synthetic seismograms determine the high frequency corner in our waveform comparisons to 1 Hz. The low frequency corner for the waveform comparisons is set at 0.05 Hz because ground motions with periods longer than 20 s are seldom considered in seismic hazard analyses. Broadband instruments permit waveform comparisons in the 0.05-1.0 Hz frequency band. Signal quality from the strong motion instruments, however, is poor below 0.5 Hz, and comparisons between the observed and synthetic seismograms for these instruments are limited to the 0.5-1.0 Hz frequency band. Since good-quality strong-motion data is available only for the Randolph earthquake, and much of the data is restricted to the vertical-component, we analyze the 0.5-1.0 Hz frequency band for the Randolph earthquake in a separate section.

Table 1: Summary of scenario earthquake parameters

Event	Date	Lon	Lat	Depth(km)	Mw	strike	dip	rake
Ephraim	20071105	-111.64	39.36	15	3.76	230	25	-65
Randolph	20100415	-111.10	41.70	5	4.51	210	35	-45
Tremonton	20070901	-112.33	41.64	9	3.66	245	85	5

Goodness-of-fit characterization

We characterize goodness-of-fit (GOF) between the observed and simulated seismograms using the GOF measure of Olsen and Mayhew (2010). The parametric GOF values (GOF_p) for each of the seven waveform parameters from the synthetic and observed seismograms (p_S and p_O, respectively) are calculated with the complementary error function (erfc):

$$GOF_p = 100 \text{ erfc}(2 |p_S-p_O|/(p_S+p_O)) \tag{5}$$

GOF values are calculated using seven waveform parameters recommended by Olsen and Mayhew (2010): (1) peak ground displacement (PGD), (2) peak ground velocity (PGV), (3) peak ground acceleration (PGA), (4) cumulative energy (E), (5) energy duration (DUR), (6) spectral acceleration amplitudes (SA), and (7) Fourier spectral amplitudes (FS). These parameters were selected because of their importance to the seismic hazard community. In analysis of the earthquake simulations, we distinguish between the "parameter" and "full" GOF. Parameter or parametric GOF values are calculated as in Eqn. 5; the full GOF values are the equal-weighted arithmetic mean values of the parametric GOF values for the seven parameters listed above. The resulting GOF values range from 0-100, where a value of 100 represents a perfect fit between the recorded and synthetic waveforms. Olsen and Mayhew (2010) characterize fits above 85 as excellent; from 65-85 as good; from 45-65 as fair. GOF values below 45 are deemed poor.

RESULTS

Earthquake simulations with the WCVM

We simulated the set of scenario earthquakes to a maximum frequency of 1.0 Hz using the WCVM as the material model and retrieve earthquake ground motions at the locations of the broadband and strong-motion seismographs within the simulation domain. For the Ephraim, Randolph and Tremonton earthquakes, 66, 72 and 38, respectively, 3-component records are available from individual seismographs. Of these seismographs, 17, 6 and 11, record broadband ground motions, respectively. The paucity of permanent broadband stations within the simulation domain and the infrequency of earthquakes that release sufficient energy to produce ground motions with good quality for comparison purposes generally limit our data analysis to the broadband earthquake records. In addition, station siting considerations for low seismic noise result in no broadband seismographs being located within the sedimentary basins of the WCVM. Many of the strong-motion instruments are located within the basins or near the basin-edges, and can provide additional information at higher frequencies (0.5-1.0 Hz), however only the records from the Randolph earthquake have good signal and are analyzed.
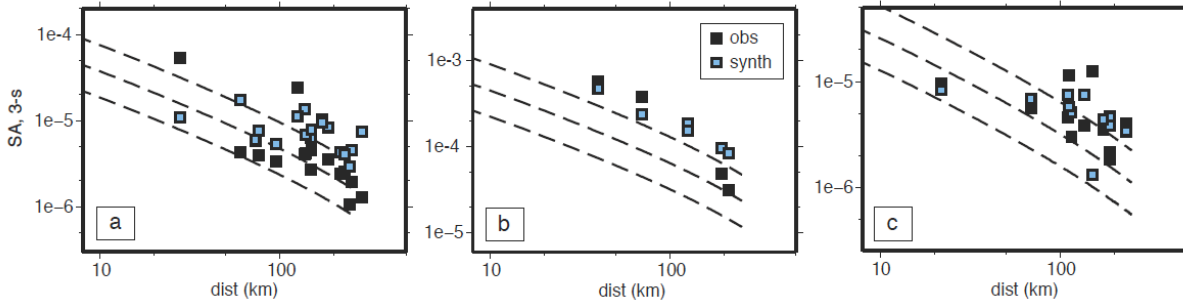
Fig. 3. Comparison of spectral accelerations at 3 s period from the earthquake records, synthetics and the Boore and Atkinson (2008) GMPE (BC site) for the (a) Ephraim, (b) Randolph and (c) Tremonton earthquakes. Values derived from the observed and synthetic seismograms are plotted in black and blue squares, respectively. The median and one-sigma GMPE predictions are plotted with dashed black curves. Values are measured only for broadband stations.
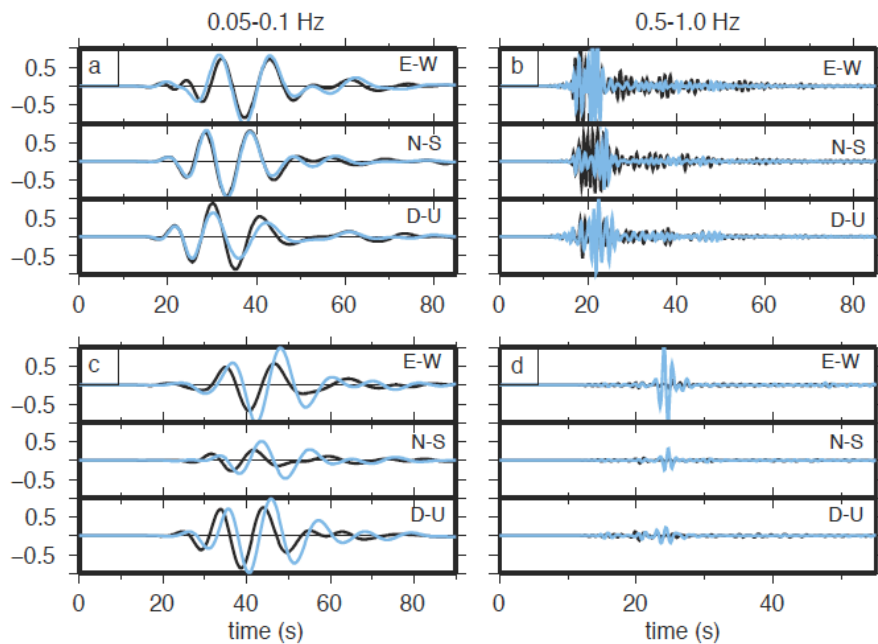

Fig. 4. Examples of waveform fit from earthquake simulations using the WCVM. Synthetic and observed seismograms are plotted in blue and black, respectively. The frequency bands used for filtering are 0.05-0.1 Hz (a,c) and 0.5-1.0 Hz (b,d). (a) Seismograms from the Randolph earthquake at station HWUT are plotted in (a) and (b) and have full GOF values of 79.9 and 76.9, respectively. Seismograms from the Ephraim earthquake at station P15A are plotted in (c) and (d) and have corresponding full GOF values of 57.4 and 27.5.

Spectral accelerations (SA) at 3 s period calculated from the three scenario earthquakes display strong variability in their ground motions with respect to the GMPE-predicted values (see Fig. 3) (Boore and Atkinson, 2008). The SA values from the Randolph and Tremonton earthquakes are largely greater than the median GMPE values; for the Randolph event, most measurements are greater than the +1-sigma GMPE estimates. Measurements from the Ephraim earthquake are primarily distributed within the uncertainty estimates of the GMPE values. Comparison of the observed SA at 3 s period with the GMPE predictions shows that the GMPE estimates fail to capture the variation in the SA ground motions with distance for the WF region. The inability of the reference GMPE to predict all SA values as a function of distance is particularly notable for the Randolph and Tremonton earthquakes. Because of the complex earth structure and wave propagation that occur in the WF, and which may be pronounced in the sedimentary basins, deterministic earthquake simulations may be a more appropriate means to predict earthquake ground motions.

GOF calculations, f≤1.0 Hz.

We calculate parametric GOF values associated with the waveform parameters (PGD, PGV, PGA, E, DUR, SA and FS) in the 0.05-0.1, 0.1-0.2, 0.2-0.5 and 0.5-1.0 Hz frequency bands. Examples of the observed and synthetic seismograms at two different frequency bands are given in Fig. 4, along with the full GOF values.
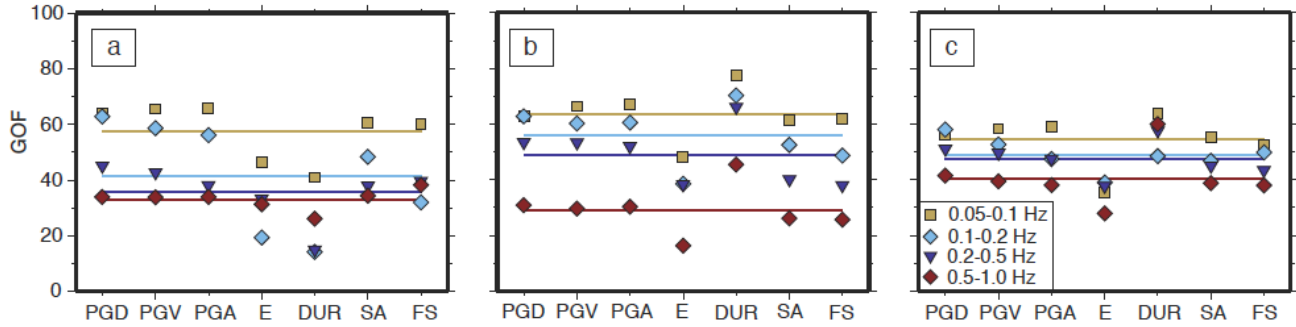

Fig. 5. Parametric and full GOF values from the (a) Ephraim, (b) Randolph and (c) Tremonton earthquake simulations using the WCVM. Parametric GOF values are computed for the 0.05-0.1 Hz (cyan squares), 0.1-0.2 Hz (magenta diamonds), 0.2-0.5 Hz (blue triangles) and 0.5-1.0 Hz (red diamonds) frequency bands. The full GOF values for each frequency band are plotted as solid lines.

For all scenario earthquakes, the full GOF values decrease as the frequencies of the measurements increase. Parametric GOF values generally show the same trends with frequency, however, several parametric GOF values show exceptions. The parametric and full GOF values are plotted in Fig. 5. For all events, the parametric GOF values associated with the peak ground parameters (PGD, PGV and PGA) are larger than the full GOF values at all frequency bands, and the cumulative energies (E) are lower than the full GOF values at all frequency bands. The Randolph and Tremonton events exhibit similar patterns for energy durations (DUR) and the amplitudes of the response (SA) and Fourier spectra (FS), with the energy durations having better fits than the full GOF and the spectral amplitudes having similar or lower parametric GOF values than the full GOF. For the Ephraim event, the opposite patterns are largely observed; durations are more poorly fit than the full GOF and the spectral amplitudes are generally better fit.

Spatial variations in the full GOF values for each frequency band exhibit earthquake-specific patterns. The results from the frequency band analyses are plotted in Fig. 6. For the Ephraim earthquake, fits to the observed seismograms are generally good in the lowest frequency band (0.05-0.1 Hz), with relatively poorer fits to the east of the basin. At higher frequencies (f≥0.1 Hz), GOF values decrease markedly and the few stations that exhibit fair or better GOF values (GOF>45) are located at those points outside of the basin and at the basin edge where sedimentary deposits are shallow. The Randolph earthquake shows correlations between the full GOF values for comparisons from the frequency band 0.05-0.5 Hz with generally good fits outside of the basin structures and relatively poorer fits near the basin edges. In the 0.5-1.0 Hz frequency band, the GOF values near the basin edge become very poor (GOF<25) and an additional site outside of the basin shows a similarly poor fit from the synthetics. The GOF values from the Tremonton earthquake simulation exhibit the least variation of the three scenario earthquakes. Three stations show generally low GOF values; these include the station outside and west of the basin and the two stations at the southern end of the basin. Apart from these stations, no strong patterns of GOF appear for the Tremonton earthquake simulations.

To investigate the dependence of the waveform parameters on distance, we calculate R^2 for linear fits to the log-ratio waveform parameters, for the vertical-components, plotted as a function of distance. Log-ratio values are calculated as the natural logarithm of the ratio of the synthetic to observed waveform parameters, $\ln(p_{syn}/p_{obs})$, where p_{syn} and p_{obs} refer to the synthetic and observed waveform parameters (e.g., PGV). In contrast to the parameter GOF values, which quantify the fit but give no indication of bias, the log-ratio values indicate the relative values of the observed and synthetic parameters. Good correlations between distance and the log-ratios of peak ground velocity and acceleration are observed from the Ephraim and Randolph earthquakes. The distance-log-ratio correlations from the two earthquakes exhibit different behavior and suggests that multiple factors may contribute to the inability of the synthetic seismograms to predict ground motions. The Randolph earthquake fits are generally good at close distances and degrade with increasing distance, with the simulated ground motions giving larger values than the observed records. For the Ephraim earthquake, the simulated ground motions are too low at close distances, match the observations near 150 km distance and are too high are further distances. Since the Ephraim and Randolph earthquake hypocenters are located well outside of the sedimentary basins and result in many paths that propagate through the regional model, the poor fits to the peak ground motions in the higher frequency bands suggests that material properties of the regional model or un-modeled basins outside of the WCVM may cause the observed data misfits. Poorly-modeled seismic impedance boundaries may also contribute to the discrepancies in peak ground motions. No

correlations between the waveform parameter log-ratios and distance are observed for the Tremonton earthquake. The PGV log-ratios are plotted as a function of distance in Fig. 7.
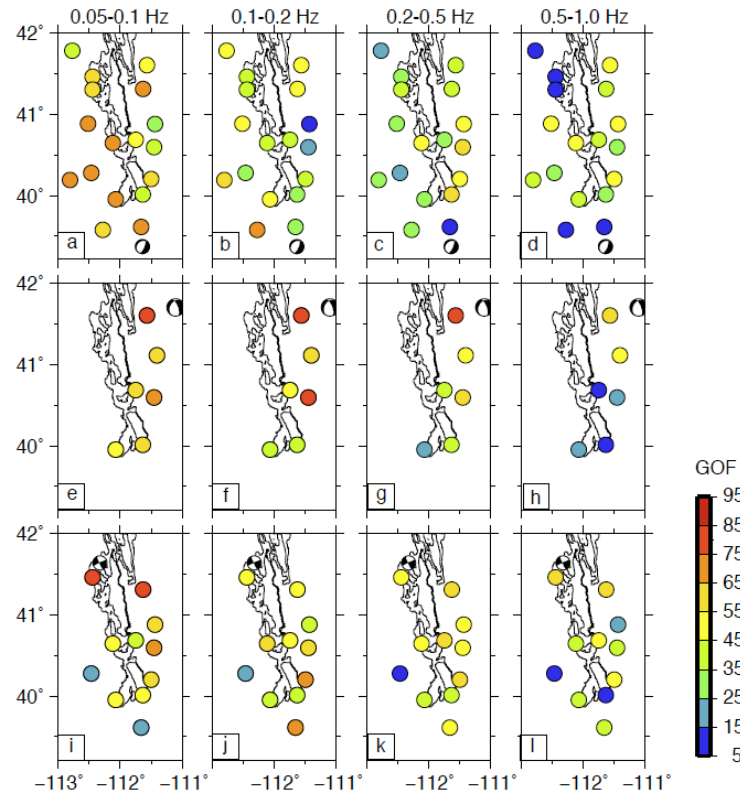

Fig. 6. Spatial variation in full GOF values from (a-d) Ephraim, (e-h) Randolph and (i-l) Tremonton earthquake simulations with the WCVM measured in the frequency bands (a/e/i) 0.05-0.1 Hz, (b/f/j) 0.1-0.2 (c/g/k) 0.2-0.5 and (d/h/l) 0.5-1.0 Hz. Earthquake locations and focal mechanisms are denoted with beachball plots.
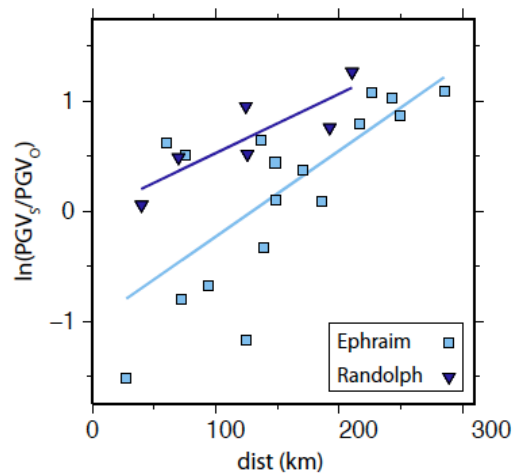

Fig. 7. Variation in the log-ratio of PGV from synthetic and observed seismograms with distance. Calculated log-ratios from the Ephraim and Randolph earthquake simulations are plotted with light blue squares and dark blue triangles, respectively. Different frequency bands are plotted for the two earthquakes. Log-ratio values from the Ephraim event are calculated from the 0.5-1.0 Hz frequency band; the values from the Randolph event correspond to the 0.2-0.5 Hz frequency bands. Linear fits to the measurements are plotted with solid lines. The calculated R^2 values are 0.71 and 0.85 and suggest a correlation between the parameters and distance.

Mean GOF values for the Ephraim, Randolph and Tremonton earthquakes in the 0.05-0.1, 0.05-0.2, 0.05-0.33, 0.05-0.5 and 0.05-1.0 Hz frequency bands are calculated and presented in Table 2. We calculate the full GOF values for theses broader band measurements (between 0.05 Hz and various high frequency corners) because these bands better represent the overall goodness-of-fit expected from broadband waveform modeling. Using the Mayhew and Olsen (2010) waveform fit designations, where GOF values of 45 correspond to a fair waveforms fit, we find that the fit of the synthetics to the observed seismograms is good, declining to only fair at upper pass-band frequencies of 0.1 Hz for the Ephraim earthquake and 0.5 Hz for the Randolph and Tremonton earthquakes.

Randolph earthquake GOF, using broadband and strong-motion instruments, 0.5≤f≤1.0 Hz.

We examine the GOF calculations from the Randolph earthquake simulation in the 0.5-1.0 Hz frequency band separately because this event is the only earthquake simulated in this study for which high signal-to-noise records are available from the strong-motion instruments within the sedimentary basins. The incorporation of the strong-motion instruments provides additional data constraints and better direct sampling of the response of the basin to earthquake ground motions. Because many of the strong-motion instruments record only vertical motions, the results from the measurements cannot be directly compared with the results utilizing only broadband stations.

Spatial variations in the full GOF and in the log-ratios of PGV and energy duration exhibit strong spatial patterns. Results are plotted in Fig. 8. The GOF values from the 0.5-1.0 Hz frequency band indicate generally fair to poor waveform fits, with the best-fitting synthetics corresponding to stations located outside of the basin and in locations where sediment thicknesses are low. The poorest waveform fits exist at those stations located near to the basin edge, particularly where steeply dipping sediment-basement interfaces exist, and in regions with thick sediment overburden. In addition to the full GOF values, we analyze the log-ratios ($r_{le}=\ln(p_{syn}/p_{obs})$) of the waveform parameters, PGV and DUR. The Randolph earthquake simulation almost uniformly over-predicts PGV and under-predicts energy durations. Over-prediction of PGV is particularly pronounced ($r_{le}>1$) near the basin edges and for regions of the model where thick sediments exist. Discrepancies in energy duration are greatest ($r_{le}<-1$) over a more confined region, restricted to the Salt Lake Basin, as well as several sites at the sedimentary basin edge and a station located in a region of high topography. At the vast majority of sites with greatly under-predicted energy durations ($r_{le}<-1$), PGV is greatly over-predicted ($r_{le}>1$) by the simulation.

Table 2: Summary of GOF values from simulated earthquakes in five frequency bands.

f (Hz)	Ephraim	Randolph	Tremonton
0.05-0.1	57.3	63.4	53.5
0.05-0.2	43.3	56.8	52.0
0.05-0.333	42.5	55.2	51.7
0.05-0.5	38.4	49.8	50.0
0.05-1.0	35.5	34.1	43.9

Earthquake simulations with alternate material models

We repeat the earthquake simulations for the set of scenario earthquakes to a maximum frequency of 0.5 Hz using the alternate material models: (1) WCVM-ANT, in which the regional velocity model is replaced with a seismic velocity model derived from ambient noise tomography (Moschetti et al., 2010); (2) WCVM-b1, in which the deep basin seismic velocities are reduced by 10%; we define the deep basin as the volume bounded by the R1 and R3 surfaces; and (3) WCVM-b2, in which the deep basin velocities are increased by 10%. The perturbations to the deep basin seismic velocities are consistent with the range in *k* values from Faust's relation (Eqn. 1).

All GOF computations are repeated, as described above, for the waveforms from the earthquake simulations using the alternate material models. Fig. 9 displays the full GOF values as percent difference relative to the values computed from WCVM simulations. No alternate model results in an increase in the full GOF for all earthquakes and all period bands. Somewhat surprisingly, modifications in the material model result in full GOF value perturbations of less than 5%. Significantly larger perturbations to individual parametric GOF values exist, however, we aim to minimize the overall misfit of the synthetic seismograms to the observed records. The greatest improvements in the full GOF values for the Ephraim, Randolph and Tremonton earthquake simulations are achieved with the alternate material model WCVM-b1, for which the deep basin seismic velocities are reduced by 10%. This model gives full GOF values for the simulated earthquakes of 39.0, 52.2 and 48.7 for the 0.05-0.5 Hz frequency band. Although these values

are between 0.5-2.5% larger than the GOF values for the earthquake simulations using the WCVM, the Ephraim earthquake ground motions are still poorly fit.
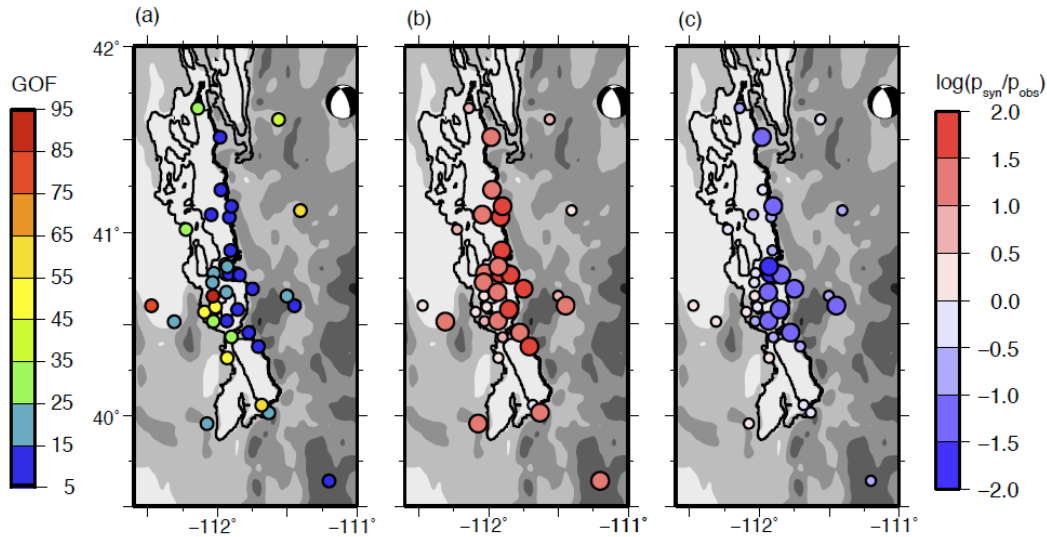

Fig. 8. Spatial variation in (a) full GOF and log-ratios in (b) PGV and (c) energy duration from the Randolph earthquake simulation in the frequency band 0.5-1.0 Hz. Only vertical-component data is utilized. Full GOF is calculated as described in the text, but using only vertical-component data. Larger symbol sizes, in panels (b) and (c), are used for absolute log-ratio values greater than one. Black contour lines in panels (a), (b) and (c) indicate sediment depths of 5 and 1000 m.
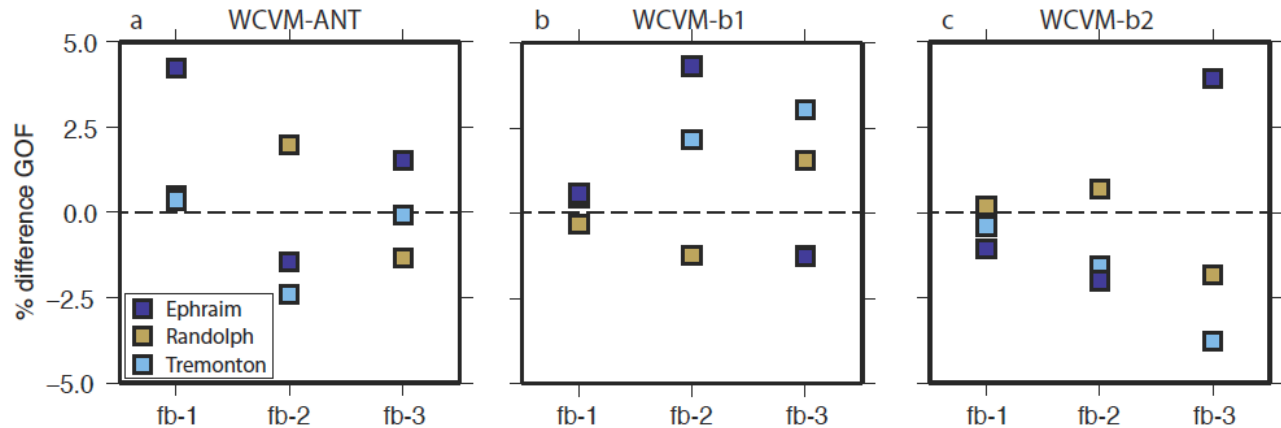

Fig. 9. Full GOF values for the Ephraim, Randolph and Tremonton earthquake simulations using the alternate material models: (a) WCVM-ANT, (b) WCVM-b1 and (c) WCVM-b2. GOF values are calculated in the frequency bands: 0.05-0.1 Hz (fb-1), 0.1-0.2 Hz (fb-2) and 0.2-0.5 Hz (fb-3). Values are presented as the percent difference from the full GOF values for the earthquake simulations using the WCVM.

CONCLUSIONS

Simulations of three small earthquakes (M: 3.6-4.5) were carried out using the WCVM to quantitatively measure the fit between observed and recorded ground motions in the Wasatch Front region below 0.5 Hz frequency. Overall, we find that the WCVM can reproduce the waveform parameters that are of greatest interest in seismic hazard studies to a fair degree, up to a high-frequency corner of 0.5 Hz for two of the simulated earthquakes and to 0.1 Hz for one of the events. There is a high degree of variability in the parametric GOF values, with peak ground motions and energy durations generally exhibiting GOF values that are larger than the full GOF measure and cumulative energy generally falling below the full GOF value. Spatial variation in the GOF is high but generally

poorer fits are observed at the seismographs located above thick sediments and near basin-edges. Regional patterns of higher and lower GOF are observed; however, these regions appear to be event-specific and may result from complex wave propagation due to seismic velocity structures that are poorly modeled in the WCVM. Discrepancies between the GOF values from different earthquake simulations may reflect the accuracy of the hypocenters and focal mechanisms; this paper has assumed these estimates are correct for the earthquake modeling. In addition, the Ephraim and Randolph earthquakes exhibit a correlation between distance and the discrepancies in peak ground motions (velocity and acceleration) for the observed and synthetic seismograms at frequencies above 0.2 Hz. Future investigations of seismic attenuation may improve these results.

We tested the ability of three alternate material models, derived by simple perturbations to the WCVM, to improve GOF estimates at frequencies below 0.5 Hz. Improvements in the calculated GOF values from the alternate models are observed in multiple frequency bands, and the alternate model for which the seismic velocities in the deep basin are reduced by 10% gives almost uniform improvements in GOF below 0.5 Hz. However, the GOF improvements from these alternate models are not significant, and we suggest that there is no compelling evidence to modify the WCVM with similar perturbations at this time. Because the alternate models predict ground motions from the simulated earthquakes at a GOF level comparable to the WCVM, these models may be used in future modeling scenarios to provide additional constraints on earthquake ground motion uncertainties associated with potential earthquakes in the Wasatch Front.

REFERENCES

Bashore, W.M. [1982], Upper crustal structure of the Salt Lake Valley and the Wasatch fault from seismic modeling, M.S. Thesis, University of Utah, Salt Lake City, Utah, 95 pp. 6 plates.

Boore, D. M. and G. M. Atkinson [2008], Ground-motion prediction equations for the average horizontal component of PGA, PGV, and 5%-damped PSA at spectral periods between 0.01 and 10.0 s. Earthquake Spectra, Vol. 24, No. 1, pp. 99-138.

Brocher, T. [2006], Key Elements of Regional Seismic Velocity Models for ground motion simulations, Proc. of Int. Workshop on Long-Period Ground Motion simulations and velocity structures, Tokyo, Nov 14-15, 2006.

Faust, L. Y. [1951], Seismic velocity as a function of depth and geologic time, Geophys. Vol. 16, pp. 192-206.

Frankel, A., W. J. Stephenson, D. L. Carver, R. A. Williams, J. K. Odum and S. Rhea [2007], Seismic hazard maps for Seattle, WA incorporating 3D sedimentary basin effects, nonlinear site response, and rupture directivity, US Geological Survey Open File Report 2007-1175.

Frankel, A., D. Carver, E. Cranswick, T. Bice, R. Sell, and S. Hanson [2001], Observations of basin ground motions from a dense seismic array in San Jose, California, Bull. Seism. Soc. Am. Vol. 91, pp. 1–12.

Herrmann, R. B., H. Benz and C.J. Ammon [2011], Monitoring the earthquake source process in North America. Bull. Seismol. Soc. Am. in press

Liu, Q., R. J. Archuleta and R. B. Smith [2010], Ground motion from dynamic ruptures on the Wasatch Fault embedded in a 3-D velocity structure. Seism. Res. Lett. Vol. 81, No. 2, pp. 320.

Lund, W. R. [2005], Consensus preferred recurrence-interval and vertical slip-rate estimates: Review of Utah paleoseismic-trenching data by the Utah Quaternary Fault Parameters Working Group. Utah Geological Survey, Bull. Vol. 134.

Mabey, D.R. [1992], Subsurface geology along the Wasatch Front, in Assessment of Earthquake Hazards and Risk Along the Wasatch Front, Utah, P.L. Gori and W.W. Hays (Editors), U.S. Geol. Surv. Pro. Pap. 1500-A-J, C1-C16.

Magistrale, H., S. Day, R. W. Clayton, and R. Graves [2000], The SCEC southern California reference three-dimensional seismic velocity model version 2, Bull. Seismol. Soc. Am., Vol. 90, No. 6B, pp. S65-S76.

Magistrale, H., K. Olsen and J. Pechmann [2008], Construction and Verification of a Wasatch Front Community Velocity Model: Collaborative Research with San Diego State University and the University of Utah. Final Technical Report, USGS 06HQGR0012.

Mattick, R. E. [1970], Thickness of unconsolidated to semiconsolidated sediments in JordanValley, Utah, U.S. Geol. Surv. Pro. Pap. 700-C, C119-C124.

McCalpin, J.P., and S. P. Nishenko [1996], Holocene paleoseismicity, temporal clustering, and probabilities of future large (M>7) earthquakes on the Wasatch fault zone, Utah. J. Geophys. Res., Vol. 101, pp. 6233-6253.

McNeil, B.R., and R.B. Smith [1992], Upper crustal structure of the northern Wasatch Front,Utah, from seismic reflection and gravity data, Utah Geol. Surv. Contract Rept. 92-7, 62 pp.,

Moschetti, M.P. and L. Ramirez-Guzman [2011], Testing the Wasatch community velocity model with long period (T > 2 s) ground motion simulations. Seism. Res. Lett. Vol. 82, No. 2.

Moschetti, M. P., M. H. Ritzwoller, F.-C. Lin, and Y. Yang [2010], Crustal shear wave velocity structure of the western United States inferred from ambient seismic noise and earthquake data, J. Geophys. Res. Vol. 115, No. B10306.

O'Connell, D. R. H., S. Ma and R. J. Archuleta [2007], Influence of Dip and Velocity Heterogeneity on Reverse- and Normal-Faulting Rupture Dynamics and Near-Fault Ground Motions. Bull. Seism. Soc. Am., Vol. 97, No. 6, pp. 1970-1989.

Olsen, K. B. and J. E. Mayhew [2010], Goodness-of-fit Criteria for Broadband Synthetic Seismograms, with Application to the 2008 Mw 5.4 Chino Hills, California, Earthquake, Seism. Res. Lett. Vol. 81, No. 5, pp. 715-723

Olsen, K. B., J.C. Pechmann, J. C., and G.T. Schuster [1995], Simulation of 3D elastic wave propagation in the Salt Lake Basin. Bull. Seism. Soc. Am., Vol. 85, No. 6, pp. 1688-1710.

Petersen, M., A. Frankel, S. Harmsen, C. Mueller, K. Haller, R. Wheeler, R. Wesson, Y. Zeng, O. Boyd, D. Perkins, N. Luco, E. Field, C. Wills and K. Rukstales [2008], Documentation for the 2008 update of the United States national seismic hazard maps, U.S. Geological Survey Open-File Report 2008-1128.

Ramirez-Guzman, L., O. S. Boyd, S. Hartzell and R. A. Williams [2010], Earthquake Ground Motion Simulations in the Central United States, AGU, Abstract S53D-06

Roten, D., K.B. Olsen, J.C. Pechmann, V.M. Cruz-Atienza and H. Magistrale [2010], Ground motion predictions from 0-1.0 Hz for M7 earthquakes on the Salt Lake City Segment of the Wasatch Fault, Utah. Seism. Res. Lett. Vol. 81, No. 2, pp. 320.

Suss, M. P., and J. H. Shaw [2003], P wave seismic velocity structure derived from sonic logs and industry reflection data in the Los Angeles basin, California, J. Geophys. Res., Vol. 108, No. B3.

Stephenson, W.J. [2007], Velocity and density models incorporating the Cascadia subduction zone for 3-D ground motion simulations. US Geological Survey Open File Report, pp 28.

Taborda, R. and J. Bielak [2010], Three Dimensional Nonlinear Soil and Site-City Effects in Earthquake Simulations, AGU Abstract S51A-1923.

Tu, T., H. Yu, L. Ramirez-Guzman, J. Bielak, O. Ghattas, K.-L. Ma and D. R. O'Hallaron [2006], From mesh generation to scientific visualization: an end-to-end approach to parallel supercomputing. ACM/IEEE.